Optical and Electrical Characterization of 4,6-Diacetylresorcinol and 4,6-Bis(1-hydrazonoethyl)benzene-1,3-diol and Their Photo-Applications

S.S. Shenouda[a,b,*], M. Shebl[c], H.S. Hafez[d] and M. Saif[d]

[a] *Physics Department, Faculty of Education, Ain Shams University, Roxy, 11341, Cairo, Egypt*
[b] *Department of Basic Sciences, Obour High Institute for Engineering and Technology, 11837, Cairo, Egypt*
[c] *Chemistry Department, Faculty of Education, Ain Shams University, Roxy, 11341, Cairo, Egypt*
[d] *Nano-Photochemistry and its Environmental Applications Laboratory, Environmental Studies and Research Institute (ESRI), University of Sadat City, Sadat City, 23897, Menofia, Egypt*

Received: 09.05.2023 & Accepted: 15.06.2023

Doi: 10.12693/APhysPolA.144.128 *e-mail: shenouda.fam@edu.asu.edu.eg

In this research, we provide the first optical and electrical characterization of 4,6-diacetylresorcinol and 4,6-bis(1-hydrazonoethyl)benzene-1,3-diol. The optical properties have been studied by measuring the diffused reflectance. Both materials have indirect optical transitions with energy gaps of 1.91 and 1.83 eV, respectively. AC electrical conductivity of both materials increases with increasing the applied frequency (1 kHz–5 MHz). It obeys $\sigma_{ac}(\omega) = B\omega^S$ with S about unity and is explained in terms of correlated barrier hopping model. 4,6-Diacetylresorcinol has higher values of AC conductivity and dielectric constant than those of 4,6-bis(1-hydrazonoethyl)benzene-1,3-diol. Finally, 4,6-bis(1-hydrazonoethyl)benzene-1,3-diol could be employed as a dye to form dye-sensitized solar cells for photosensing applications.

topics: 4,6-diacetylresorcinol (DAR), 4,6-bis(1-hydrazonoethyl)benzene-1,3-diol (BHEBD), diffused reflectance, dielectric properties

1. Introduction

Compounds under investigation, namely 4,6-diacetylresorcinol (DAR) and 4,6-bis(1-hydrazonoethyl)benzene-1,3-diol (BHEBD) (see Fig. 1), have been prepared, characterized, and used as chelating agents towards alkaline earth metal cations: Mg(II), Ca(II), Sr(II), and Ba(II) and transition metal cations: Cu(II), Ni(II), and Co(II) [1–4]. Also, they have been used as starting materials for the construction of polydentate ligands, which were used in the synthesis of polynuclear (mononuclear, homo- and hetero-binuclear) complexes [5-17].

The importance of poly-nuclear complexes arises from their fascinating magnetic characteristics, such as the single-molecule magnet (SMM) properties [18]. Also, they are used as forerunners of molecule-based magnetic materials [19–22]. Indeed, polynuclear complexes are of immense interest not only in the elucidation of the magnetic exchange between metal ions but also as models of the active sites of multi-metalloenzymes [23, 24]. Finally, polynuclear

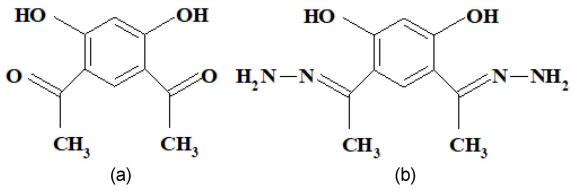

Fig. 1. Structure of (a) 4,6-diacetylresorcinol (DAR), (b) 4,6-bis(1-hydrazonoethyl)benzene-1,3-diol (BHEBD).

complexes derived from 4,6-diacetylresorcinol and 4,6-bis(1-hydrazonoethyl)benzene-1,3-diol have attracted considerable interest in inorganic and bioinorganic chemistry as a result of their biological applications, including antimicrobial [11–13], antioxidant [14, 16], and antitumor [10, 14, 17] properties.

To the best of our knowledge, no reports on the optical, electrical, and dielectric characteristics of these materials have been carried out. Thus, this research aims to characterize such materials. The

optical properties are important for determining the optical transition and the value of the energy gap by measuring and analyzing the diffused reflectance of the samples [25]. Also, the AC electrical conductivity is important for determining and understanding the conduction mechanisms under the influence of the AC field [25, 26]. The dielectric properties are also essential to understand the nature of dielectric loss and to develop passive devices for integrated circuits [25, 27]. Different characterizations have been employed to include the behavior of the materials under a wide range of wavelengths with the available instruments. Furthermore, the materials are employed as dyes to form dye-sensitized solar cells (DSSCs) for photosensing applications. Recently, DSSCs have attracted much attention owing to their low cost, easy preparation, environmental friendliness, non-toxicity, and relatively high efficiency [28, 29]. Generally, DSSC has four main components: photoanode, photosensitizer, electrolyte, and counter electrode [28, 30]. We intended to replace the expensive common photosensitizer (ruthenium complex) with the investigated compounds (DAR and BHEBD). Finally, the dependence of short circuit current density on the illumination intensity has been investigated to check the photosensitivity mechanism of the DSSC.

2. Experimental technique

4,6-Diacetylresorcinol was prepared by acetylation of resorcinol with acetic anhydride in the presence of excess zinc chloride, as reported in detail in [1]. 4,6-Bis(1-hydrazonoethyl)benzene-1,3-diol was prepared by condensation of 4,6-diacetylresorcinol with hydrazine hydrate in molar ratio 1:2 (diacetylresorcinol:hydrazine) in methanol, as described in detail in [2]. The samples have been compressed to form circular discs with a thickness of 1 mm and a radius of 13 mm. Diffused reflectance of the samples has been measured in the wavelength range of 220–750 nm using a UV/VIS spectrophotometer (JASCO V-550). The impedance, loss tangent and capacitance of the samples have been measured using the computerized HIOKI 3532-50 LCR HiTESTER. The disk sample was placed in a special holder with two circular electrodes. The upper electrode has a smaller cross-section area used as the effective area (A) to calculate the AC conductivity and dielectric constant.

Each of the two compounds was dissolved in isopropanol. Then, TiO_2 electrodes were immersed in the two solutions for 24 h. After that, the electrodes were washed with pure ethanol and dried in air. Iodide electrolyte was placed between the sensitized TiO_2 electrode and a sputtered Pt/FTO counter electrode to form DSSC. The photovoltaic characteristics of both cells were measured using computerized Keithley source-measure (K2635, USA), solar power meter (TM-206, Tenmars, Taiwan), and a xenon lamp (CHF-XM500, Trusttech Co., Ltd. — China) at room temperature. Details of the preparation and characterization of the electrodes and the cells are in our previous work [31].

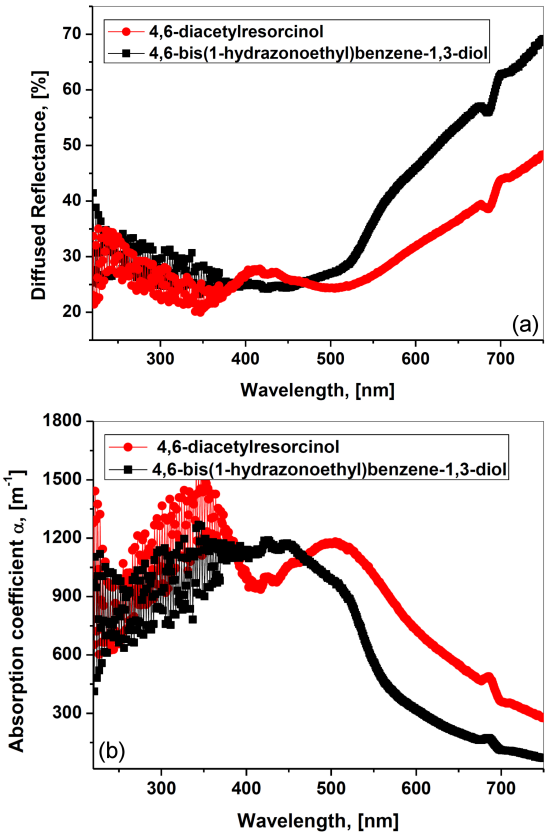

Fig. 2. Wavelength dependence of (a) diffused reflectance, (b) absorption coefficient for 4,6-diacetylresorcinol and 4,6-bis(1-hydrazonoethyl)benzene-1,3-diol.

3. Results and discussion

3.1. Optical properties

To investigate the optical properties of 4,6-diacetylresorcinol and 4,6-bis(1-hydrazonoethyl)benzene-1,3-diol, the diffused reflectance R_d of both samples was measured, as seen in Fig. 2a. The diffused reflectance is the reflected light from powder samples. The basic equation describing this process is given by [32, 33]

$$-\frac{1}{\rho k}\frac{\mathrm{d}I}{\mathrm{d}S} = I - \frac{j}{k}, \tag{1}$$

where I is the intensity of the incident light, ρ is the medium density, k is an attenuation coefficient due to absorption and scattering, $\mathrm{d}S$ is the change of the pathlength, and j is the scattering function. The solution to this equation was suggested by Schuster and developed by Kubelka and Munk. Thus, this solution is called Schuster–Kubelka–Munk theory with the following function [32, 33]

$$F(R_d) = \frac{(1-R_d)^2}{2R_d}. \quad (2)$$

Then, the absorption coefficient could be determined using the measured diffused reflectance R_d as follows [32–34]

$$\alpha = \frac{F(R_d)}{t} = \frac{1}{t}\,\frac{(1-R_d)^2}{2R_d}, \quad (3)$$

where t is the thickness of the sample. The wavelength dependence of the absorption coefficient is presented in Fig. 2b. Clearly, there are strong and weak absorption bands for both molecules. The high energy (strong) absorption band is assigned to π–π^* transitions, while the lower energy (weak) band is assigned to the n–π^* transitions.

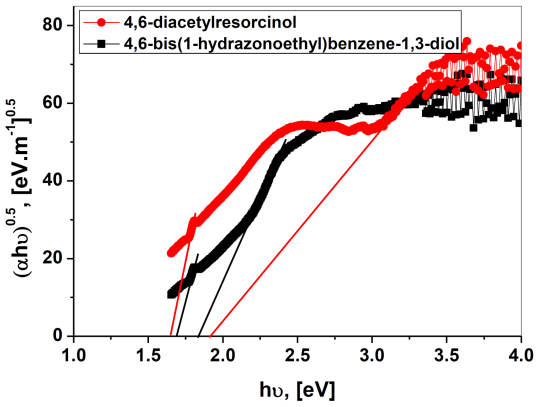

Fig. 3. Dependence $(\alpha h\nu)^{0.5}$ vs $h\nu$ for 4,6-diacetylresorcinol and 4,6-bis(1-hydrazonoethyl)benzene-1,3-diol.

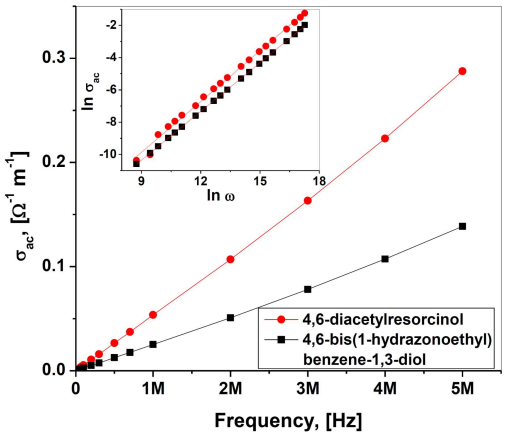

Fig. 4. Dependence of the AC conductivity on the frequency of the applied field. Inset: $\ln(\sigma_{ac})$ vs $\ln(\omega)$ of 4,6-diacetylresorcinol and 4,6-bis(1-hydrazonoethyl)benzene-1,3-diol.

TABLE I

Value of the energy gaps of DAR and BHEBD dyes.

	E_{g1} [eV]	E_{g2} [eV]
DAR	1.65	1.91
BHEBD	1.70	1.83

The photon energy dependence of the absorption coefficient has been analyzed using the following equation to determine the optical energy gap E_g [35–37]

$$(\alpha h\upsilon) = A\,(h\nu - E_g)^m, \quad (4)$$

where A is a constant and m is a number relating to the type of the optical transition ($m = 2$ and 0.5 for indirect and direct allowed transition, respectively). It is clear from Fig. 3 ($(\alpha h\nu)^{1/2}$ vs $h\nu$) that both materials have indirect allowed transitions. The optical energy gaps of 4,6-diacetylresorcinol and 4,6-bis(1-hydrazonoethyl)benzene-1,3-diol were determined by extrapolating the linear part in Fig. 3 to the x-axis ($h\nu$). The values of the energy gaps are 1.65 and 1.91 eV for the 4,6-diacetylresorcinol and 1.70 and 1.83 eV for 4,6-bis(1-hydrazonoethyl)benzene-1,3-diol as presented in Table I. These findings suggest the semiconducting behavior of the organic materials under investigation. Thus, these materials could be employed for further applications.

3.2. Electrical properties

In order to study the electrical properties, the impedance Z of both samples has been measured at different frequencies (1 kHz–5 MHz). Then, the AC electrical conductivity σ_{ac} is calculated using the following equation [38]

$$\sigma_{ac} = \sigma_{tot.ac} - \sigma_{dc} = \frac{t}{ZA} - \frac{t}{RA}, \quad (5)$$

where R is the ohmic resistance, and A is the effective area of the measured sample (area of the upper electrode). The variation of the AC conductivity depending on the frequency is shown in Fig. 4. Clearly, the AC conductivity of DAR is higher than that of BHEBD. This could be due to the difference in the chemical structure. Also, the AC conductivity of both samples increases linearly with the frequency. Thus, these two materials obey Jonscher's universal power equation of semiconductors [39, 40]

$$\sigma_{ac} = B\,\omega^S, \quad (6)$$

where B is a constant. Now, $\ln(\sigma_{ac})$ vs $\ln(\omega)$ is plotted in the inset of Fig. 4 for both samples. The slope of both lines (S) is about unity, thus, the AC conductivity of both samples can be illustrated as correlated barrier hopping between intimate valence alternation pairs [41, 42].

3.3. Dielectric properties

In order to develop passive devices for advanced technologies, it is important to study the behavior of the dielectric constant [27]. The dielectric constant ε_1 and the dielectric loss ε_2 were calculated from the measured capacitance C and loss tangent $\tan(\delta)$ as following [25, 43]

$$\varepsilon_1 = \frac{C\,t}{\varepsilon_o A}, \quad (7)$$

TABLE II

Photovoltaic parameters of DSSC based on DAR and BHEBD dyes.

	P_{in} [mW/cm^2]	V_{oc} [V]	J_{sc} [μA/cm^2]	V_m [V]	P_m [μW/cm^2]	J_m [μA/cm^2]	FF
DAR	100	0.003	30.8	0.001	0.0184	18.35	0.199
BHEBD	20	0.226	11.5	0.165	1.22	7.40	0.470
	30	0.218	17.2	0.150	1.53	10.2	0.409
	40	0.217	22.7	0.150	2.13	14.7	0.433
	50	0.228	27.7	0.150	2.90	19.3	0.459
	60	0.236	33.9	0.170	3.92	23.1	0.490
	70	0.239	40.7	0.165	4.85	29.4	0.498
	80	0.228	46.0	0.160	5.07	31.7	0.483
	90	0.255	53.3	0.185	7.22	39.0	0.531
	100	0.243	60.4	0.175	7.49	42.8	0.510

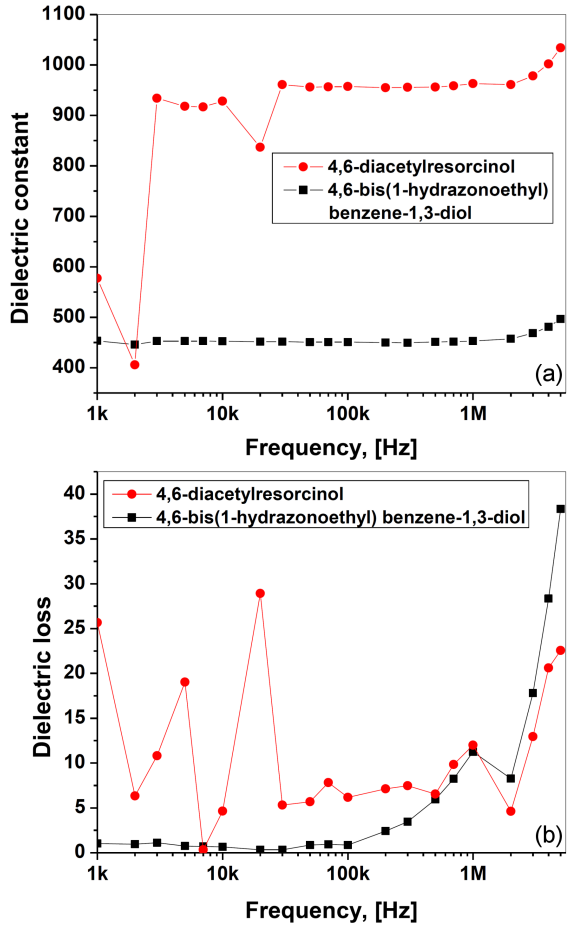

Fig. 5. Frequency dependence of (a) dielectric constant and (b) dielectric loss of 4,6-diacetylresorcinol and 4,6-bis(1-hydrazonoethyl)benzene-1,3-diol.

$$\varepsilon_2 = \varepsilon_1 \tan(\delta), \tag{8}$$

where ε_o is the vacuum permittivity. The frequency dependence of ε_1 and ε_2 for both samples is presented in Fig. 5. Clearly, the dielectric constant of DAR is higher (more than twice) than that of BHEBD in most of the frequency range. The dielectric constant seems to be frequency independent, except for a small increase after 2 MHz. This may be due to interfacial or space charge polarization at higher frequencies.

The dielectric loss of DAR is higher than that of BHEBD till 1 MHz, then the dielectric loss of DAR becomes less than that of BHEBD. The dielectric loss of BHEBD has a peak at 1 MHz, while the dielectric loss of DAR has many peaks.

3.4. Photovoltaic properties

Finally, the two compounds are employed as dyes to form dye-sensitized solar cells. The current density–voltage (J–V) of both DSSCs at 100 mW/cm^2 is presented in Fig. 6a. Clearly, the BHEBD dye shows better photovoltaic behavior. Figure 6b presents the effect of illumination intensity on the current density–voltage of the DSSC based on the BHEBD dye. The open circuit voltage (V_{oc}) and the short circuit current density (J_{sc}) were determined and listed in Table II.

Clearly, V_{oc} is approximately independent of the illumination intensity, while J_{sc} increases with increasing the illumination intensity obeying the equation [31, 44]

$$J_{sc} = \text{const } P_{in}^{\gamma}. \tag{9}$$

Here, γ is a parameter determining the recombination mechanism ($\gamma = 1$ and 0.5 for the monomolecular and bimolecular recombination mechanism, respectively). For our purpose, γ is determined from the best fitting of the relation $\ln(J_{sc})$ vs $\ln(P_{in})$, as presented in Fig. 7a. Therefore, γ has a value of 1.02 referring to the monomolecular recombination mechanism. Also, this approximate linear dependence of J_{sc} on the illumination intensity makes this cell promising for photosensing applications [28, 31, 45].

The maximum output power density P_m was determined from the power density–voltage (see Fig. 7b). The current density (J_m) and the voltage (V_m) corresponding to the maximum power density were determined and given in Table II.

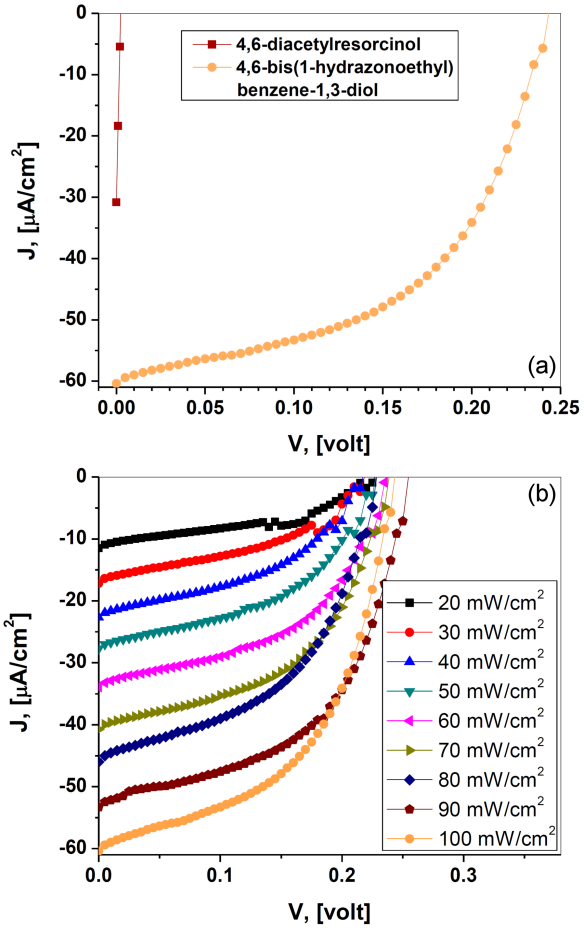

Fig. 6. Current density–voltage (J–V) of the DSSCs based on (a) DAR and BHEBD dyes at 100 mW/cm^2, (b) BHEBD at different illumination intensities.

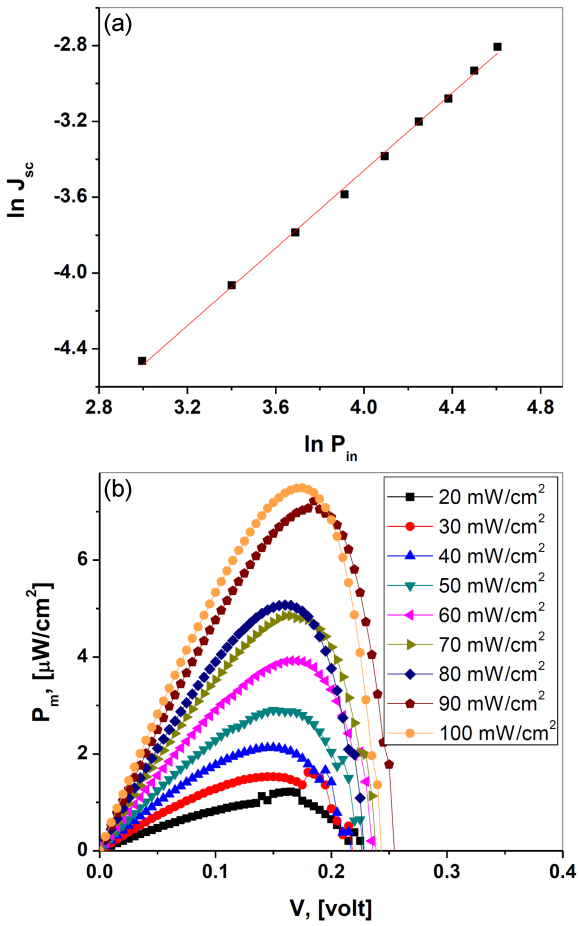

Fig. 7. (a) $\ln(J_{sc})$ vs $\ln(P_{in})$, (b) maximum power density–voltage (P_m–V) of the DSSCs based on BHEBD dye at different illumination intensities.

Other photovoltaic parameters, such as the fill factor (FF) and efficiency (η), were calculated using the following equations [31]

$$\mathrm{FF} = \frac{P_m}{J_{sc} V_{oc}}, \tag{10}$$

$$\eta = \frac{P_m}{P_{in}} \times 100\%. \tag{11}$$

The results are shown in Table II. The fill factor has a value ranging from 0.40 to 0.53, while the efficiency has a small value ($0.0065 \pm 0.0015\%$).

4. Conclusions

Both 4,6-diacetylresorcinol and 4,6-bis(1-hydrazonoethyl)benzene-1,3-diol behave like semiconductor materials. Both have indirect allowed transitions. The AC conductivity of DAR is higher than that of BHEBD. The conductivity of both materials increases linearly with increasing the applied frequency and is explained as a correlated barring hopping model. The dielectric constant of DAR is higher than that of BHEBD. The small increase of the dielectric constant at higher frequencies may be due to interfacial or space charge polarization of the molecules. The BHEBD compound could be employed as a dye to form DSSC. The linear dependence of the current density on the illumination intensity recommends this DSSC for photosensing applications.

References

[1] A.A.A. Emara, A.A.A. Abou-Hussen, *Spectrochim. Acta A* **64**, 1010 (2006).

[2] B.S. Shyamala, V. Jayatyagaraju, *Synth. React. Inorg. Met.-Org. Chem.* **33**, 63 (2003).

[3] M. Shebl, S.M.E. Khalil, A. Taha, M.A.N. Mahdi, *J. Mol. Struct.* **1027**, 140 (2012).

[4] M. Shebl, S.M.E. Khalil, A. Taha, M.A.N. Mahdi, *Spectrochim. Acta A* **113**, 356 (2013).

[5] J.H. Pandya, R.N. Jadeja, K.J. Ganatra, *J. Saudi. Chem. Soc.* **18**, 190 (2014).

[6] A.A.A. Emara, *Spectrochim. Acta A* **77**, 117 (2010).

[7] N.V. Kulkarni, M.P. Sathisha, S. Budagumpi, G.S. Kurdekar, V.K. Revankar, *J. Coord. Chem.* **63**, 1451 (2010).

[8] M. Shebl, *Spectrochim. Acta A* **73**, 313 (2009).

[9] M. Shebl, *Spectrochim. Acta A* **70**, 850 (2008).

[10] M. Shebl, *J. Coord. Chem.* **69**, 199 (2016).

[11] M. Shebl, *J. Coord. Chem.* **62**, 3217 (2009).

[12] M. Shebl, H.S. Seleem, B.A. El-Shetary, *Spectrochim. Acta A* **75**, 428 (2010).

[13] M. Shebl, M.A. El-ghamry, S.M.E. Khalil, M.A.A. Kishk, *Spectrochim. Acta A* **126**, 232 (2014).

[14] M. Shebl, *J. Mol. Struct.* **1128**, 79 (2017).

[15] K.M. Raj, B.H.M. Mruthyunjayaswamy, *Turk. J. Chem.* **37**, 775 (2013).

[16] K.M. Raj, B. Vivekanand, G.Y. Nagesh. B.H.M. Mruthyunjayaswamy, *J. Mol. Struct.* **1059** 280 (2014).

[17] S.A. Al-Harbi, M.S. Bashandy, H.M. Al-Saidi, A.A.A. Emara. T.A.A. Mousa, *Spectrochim. Acta A* **145**, 425 (2015).

[18] D. Gatteschi, R. Sessoli, *Angew. Chem. Int. Ed.* **42**, 268 (2003).

[19] H. Miyasaka, K. Nakata, K. Sugiura, M. Yamashita, R. Clérac, *Angew. Chem. Int. Ed.* **43**, 707 (2004).

[20] R. Clérac, H. Miyasaka, M. Yamashita, C. Coulon, *J. Am. Chem. Soc.* **124**, 12837 (2002).

[21] L. Lecren, O. Roubeau, O. Coulon, Y.G. Li, X.L. Goff, W. Wernsdorfer, H. Miyasaka, R. Clérac, *J. Am. Chem. Soc.* **127**, 17353 (2005).

[22] L. Lecren, W. Wernsdorfer, Y.G. Li, A. Vindigni, H. Miyasaka, R. Clérac, *J. Am. Chem. Soc.* **129**, 5045 (2007).

[23] C. Zhang, C. Zhao, Z. Ma, D. Yan, *J. Coord. Chem.* **52**, 87 (2000).

[24] A. Gleizes, M. Verdaguer, *J. Am. Chem. Soc.* **103**, 7373 (1981).

[25] S.S. Shenouda, H.Y. Zahran, I.S. Yahia, *Mater. Res. Express* **6**, 105042 (2019).

[26] N. Shukla, D.K. Dwivedi, *J. Asian Ceram. Soc.* **4**, 178 (2016).

[27] H.-M. Li, C.-H. Ra, G. Zhang, W.J. Yoo, K.-W. Lee, J.-D. Kim, *J. Korean Phys. Soc.* **54**, 1096 (2009).

[28] S.S. Shenouda, I.S. Yahia, H.S. Hafez, F. Yakuphanoglu, *Mater. Res. Express* **6**, 065004 (2019).

[29] C.-P. Lee, K.-Y. Lai, C.-A. Lin, C.-T. Li, K.-C. Ho, C.-I. Wu, S.-P. Lau, J.-H. He, *Nano Energy* **36**, 260 (2016).

[30] G. Yue, F. Li, G. Yang, W. Zhang, *Nanoscale Res. Lett.* **11**, 239 (2016).

[31] H.S. Hafez, S.S. Shenouda, M. Fadel, *Spectroch. Acta A* **192**, 23 (2018).

[32] B.M. Weckhuysen, R.A. Schoonheydt, *Catalysis Today* **49**, 441 (1999).

[33] H.Y. Zahran, S.S. Shenouda, I.S. Yahia, F. El-Tantawy, *J. Sol–Gel Sci. Technol.* **86**, 104 (2018).

[34] R. Fouad, I.A. Shaaban, T.E. Ali, M.a. Assiri, S.S. Shenouda, *RSC Adv.* **11**, 37726 (2021).

[35] J. Tauc, *Amorphous and Liquid Semiconductors*, Plenum Press, London 1974.

[36] H.M.H. Zakaly, S. Helali, O.I. Sallam, A.W. Alrowaily, N.A. Elalaily, S.A.M. Issa. *Opt. Mater.* **137**, 113504 (2023).

[37] S.S. Shenouda, M. Saif, E. Baradács, B. Parditka, T. Fodor, Z. Erdélyi, *Phys. Scr.*, **98**, 015826 (2023).

[38] A. Bouzidi, I.S. Yahia, M.S.A. El-Sadek, *Dyes Pigment* **146**, 66 (2017).

[39] A.K. Jonscher, *Nature* **267**, 673 (1977).

[40] S.I. Qashou, *Physica B Condensed Matter* **649**, 414421 (2023).

[41] S.R. Elliot, *Solid State Comm.* **27**, 749 (1978).

[42] I.S. Yahia, N.A. Hegab, A.M. Shakra, A.M. AL-Ribaty, *Physica B* **407**, 2476 (2012).

[43] I.S. Yahia, M. Shkir, S. AlFaify, V. Ganesh, H.Y. Zahran, M. Kilany, *Mater. Sci. Eng. C* **72**, 472 (2017).

[44] F. Yakuphanoglu, *J. Alloys Compd.* **494**, 451 (2010).

[45] R.K. Gupta, A.A. Al-Ghamdi, F. El-Tantawy, W.A. Farooq, F. Yakuphanoglu, *Mater. Lett.* **134**, 149 (2014).